Change On The S-Z Effect Induced By The Cooling Flow (CF) On The Hot Electronic Gas At The Center OF The Clusters Of Galaxies

Enkelejd Caca

ABSTRACT: Building more accurate profiles for temperature and density of hot electronic gas, concentrated in the center of clusters of galaxies, is a constant problem in survey of Sunyeav Zel'dovich effect (SZ). An effect that consists in the inverse Compton effect of the hot electronic gas interacting with Cosmic Microwave Back- ground (CMB) photons passing through Intra Cluster Medium (ICM). So far, the Isothermal model is used for temperature profiling in the calculation of the inverse Compton effect, but based on the recent improved observations from satellites, which showed that the hot electronic gas presents a feature, called Cooling Flow (CF). Temperatures in this model differs towards the edges of the Clusters of Galaxies, leading to a change on the Compton parameter in comparison with Isothermal model. In this paper are processed data, provided by X-ray satellite, Chandra. The X-ray analysis is based on two models for the electron density and temperature profile. A sample of 12 clusters of galaxies are analyzed, and by building the temperature profiles using CF model, the differences on the Compton parameter, are 10-100% in comparison with Isothermal model. Therefore to increase the accuracy of evaluation of the Compton parameter, we should take into account the change of the electronic gas tempera- ture, change that affect changes in both, CMB spectrum and temperature, from SZ effect.

Keywords: Cluster of Galaxies, X-ray, Comptonization, Cooling Flow, S-Z effect

1. INTRODUCTION

Over the last four decades, much effort has been put in trying to achieve the observational goal of detecting and imaging the Synyaev-Zel'dovich (SZ) effect from cluster of galaxies, first proposed in 1970s (Sunyaev and Zeldovich, 1969, 1972) as a consequence of Compton interaction between Cosmic Microwave Background (CMB) photons and highly energetic electrons present in the hot plasma of intergalactic space within cluster of galaxies (intra-cluster medium, ICM). The effect resulting in a CMB anisotropy with characteristic spectral signature and spatial correlation with cluster position in the sky, and most of of all its nearly complete indepen- dence from the cluster redshift, was soon designated as one of the most reliable and rich source of information for both cluster physics and cosmology, due to its simplest physical interpretation and marginal detection pos- sibilities even with the observation techniques and detector technology of 20 years ago. After few observation performed in the early stages of SZ search programs (Birkinshaw, 1991, 1999), the last 15 years have finally shown our capability to produce systematic SZ measurements, operating at wavelengths from a few cm to the mm/submm region, where the larger contribution to the effect is expected to fully exploit its spectral signature and thus justifies the application of multi-band techniques for good systematic control and foreground removal. While imaging of the SZ effect has already been performed at radio frequencies (Carlstrom et al., 1996; Grego et al., 1996) with the aid of interferometric detectors, higher frequency measurements have been mostly per- formed from single-pixel detectors, with the only (but significant) advantage of multi-band selection and higher spectral discrimination of the signal from unwanted contributions. Now, finally, the advance in bolometer tech- nology and the know-how of the past decades suggest that present and the near-future microwave instruments pretending to extract the largest astrophysical and cosmological information from SZ observation must be able to combine multi-frequency techniques with moderate-to-high imaging capabilities. in order to significantly reduce the bulk of systematic and statistical uncertainty coming from the modeling of ICM density and tem- perature distributions and, for ground-based experiment, take full advantage of long integration and on-site operator control to optimally customize the observation strategy. Moreover, giving the growing sky coverage capabilities of the new experiments, it will soon be possible to perform routine observations and produce un- target surveys of potentially more than 100 clusters, to determine statistically robust cosmological parameter estimates and deeply probe the universe at high red-shift. These surveys will provide a direct view of growth large scale structures and help building catalogs of cluster that will possibly extend past z ' 2 with significantly low observational biasing. This paper is organised as follows: in §2 we provide details of data reduction and, temperature and density profile. The comptonization parameter y_0 and, the change on the intensity and the temperature of the CMB are presented in §3. The result and the comparison with S-Z data are presented in §4. In §5 we provide the conclusions.

1. TEMPERATURE PROFILES

In the case of the CF clusters in order to modelling the gas temperature we use a non-isothermal model for the temperature (Piffaretti et al., 2005; Piffaretti and Kaastra, 2006; Gitti et al., 2007). The temperature declines from the maximum cluster temperature at a break radius r_{br} moving outwards and shows the characteristic temperature decline towards the X-ray emission peak. Since we are interested in the central cooling region and the cooling radius for a cooling time of 15 Gyr, R_{cool} is smaller than r_{br} for all the CF clusters, the temperature profiles can be simply modelled by a function that is monotonically raising with radius. Hence, for each cluster we select temperature bins inside the radius $R_{T,max} = r_{br}$ and fit them using the following expressions:

$$T_r = T_0 + T_1 \frac{(r/r_T)^{\mu}}{1+(r/r_T)^{\mu}} \quad (1)$$

$$\tilde{T}_r = \tilde{T}_0 - \tilde{T}_1 \exp\left(-\frac{r^2}{2r_T^2}\right) \quad (2)$$

In order to reduce the number of parameters here, we set T(r = 0) equal to the temperature of the central bin for both fits and use μ=2 in Eq.1 (Allen et al., 2001). Both temperature parameterizations (Eq. 1 and Eq. 2) are used in the computation temperature profile and in the modelling of the gas pressure, that depends from the temperature and the density of the electronic gas present at the center of the cluster. Our main results presented are achieved using the parametrization in Eq. 1, and we use the second parametrization given in Eq. 2 only in order to explore the effect of a different modelling on our main results. The changes introduced by using Eq. 2 are, quite small and do not change the results obtained by using Eq. 1. The main problem on the definition of the temperature of the gas is the correctly definition from the X-ray observation. These observations suffer from a great uncertainty. Uncertainties that depart from the way as it weighs the temperatures of the bins. Various ways to define the temperatures exist, as; spectroscopic method, spectroscopic like method (see Mazzotta et al. (2004)) etc. But this purpose, is not the goal of this work. Another uncertainty originates, also from the differences in the observations of the various detectors on same target. Another parameter to be defined is the electronic density of the gas and its profile. We model the gas density by using a single β-model given by:

$$n_r = n_0 \left(1 + \left(\frac{r}{r_c}\right)^2\right)^{-\frac{s\beta}{2}} \quad (3)$$

The density profile is fitted within $R_{n,max}$, which is the radius at the center of the last radial bin, where a robust estimate of gas density and temperature is possible (see Piffaretti et al. (2005)). An alternative parametrization of the gas density profile is the more complex double β-model (Mohr et al., 1999), which is a popular generalization of the single β-model (Cavaliere and Fusco-Femiano, 1976, 1978) used to model the central surface brightness excess observed in CF clusters.

$$n_r = n_1 \left(1 + \left(\frac{r}{r_{c1}}\right)^2\right)^{-\frac{s\beta_1}{2}} + n_2 \left(1 + \left(\frac{r}{r_{c2}}\right)^2\right)^{-\frac{s\beta_2}{2}} \quad (4)$$

Unfortunately in this case, the gas density is modeled using the sum of two single-models, so the number of free parameters is doubled: $n_{0,i}$, β_i, and $r_{c,i}$, with i = 1, 2. As a consequence, while fitting the single β-model to the density profiles gives statistically significant values for the best-fit parameters, the large number of parameters adopted in the double β-model, together with the small number of bins in which the gas density is measured, do not allow a significant determination of the best-fit parameters. Therefore, we present main results above using the single β-model (see Tab. 2). Nonetheless, in order to constrain to which extent the double β-modelling changes the results, we also fit the density profiles using a double β-model with a reduced number of fitting parameters, unfortunately only for 4 clusters (Abell 1795, Abell 1835, Abell 2204 and Abell 2390), for which we find data for the density. The derived profiles are then used to model the gas pressure as done by using the single β-model results (Fig. 2). Specially for the cluster A2004 and A2390 we use a double β-model having better results in comparison with single β-model see Fig. 2, the χ^2 for the double β-model is small than single β-model (see Tab. 4). For the first two clusters Abell 1795 and Abell 1835 single β-model and the double β-model have no difference between them and we do not need to use the second model. For all other clusters the single β-model has been assumed (r_c and density data for the β-model Tab. 3 (Bonamente et al., 2006). All parameters of this fit are showed in the table booth with the central density n_0 and r_c of the gas (Tab.3). Now, that we defined the parameters of temperature and the central electronic density we can define the pressure of the electronic gas, and in this way to define the parameter of comptonization y_0 of the CMB photons from the hot electrons present at the center of the cluster.

Table 4. *χ^2 for the two models.*

Cluster	χ^2 β-model	χ^2 double β-model
ABELL 2204	0.29	0.023
ABELL 2390	0.24	0.01

2. COMPTONIZATION PARAMETER Y

To calculate the Comptonization parameter, now we can use the temperature and density profiles obtained above. The original treatment from the (Sunyaev and Zeldovich, 1972), is based on a solution to the (Kompa- neets, 1957) equation, which is a non-relativistic (Fokker-Planck) diffusion, approximation to the exact integrals in equation 5, written for the average occupation number of the radiation energy levels:

$$\frac{\partial \bar{n}}{\partial n} = \frac{kT}{m_e c} \frac{\sigma_T n_e}{x^2} \frac{\partial}{\partial x}\left[x^4 \left(\frac{T_e}{T}\frac{\partial \bar{n}}{\partial x} + \bar{n} + \bar{n}^2\right)\right] \quad (5)$$

n_e and T_e are the electron gas temperature and number density profiles (under the assumption that the the electron population is thermally relaxed), T is the radiation temperatures (in the case of blackbody spectrum) and x is the nondimesional frequency, hv/kT. Since for the case of ICM electrons and CMB photons T_e » T = T_{CMB}, the first term in parentheses dominates over the others, allowing to reduce equation 5 to:

$$\frac{\partial \bar{n}}{\partial n} = \frac{kT_{CMB}}{m_e c} \frac{\sigma_T n_e}{x^2} \frac{\partial}{\partial x}\left[x^4 \left(\frac{T_e}{T_{CMB}}\frac{\partial \bar{n}}{\partial x}\right)\right] \quad (6)$$

A solution to this equation can be easily found under the hypothesis that the radiation field undergoes weak diffusion from the gas (i.e. multiple scattering events of a single photon are strongly unlikely), so that the right part of the equation 6 can be rewritten with the expression of a planckian occupation number for n

$$\overline{n_p}(x) = \frac{1}{e^x - 1} \quad (7)$$

Finally, integrating over the line of sight (l.o.s) through the cluster yields the non-relativistic (i.e low electron temperature) expression for the spectrum of the thermal SZ effect:

$$\Delta I_t = i_0 y g(x) \quad (8)$$

where $i_0 = 2(kT_{CMB})^3/(hc)^2$, and y is the comptonization parameter defined as:

$$y = \int_{l.o.s} n_e(l) \frac{kT_e}{m_e c^2} \sigma_T dl = \frac{kT_e}{m_e c^2} \tau \quad (9)$$

i.e. an integral of electron density and temperature profiles across the cluster; σ_T is the Thomson cross section, and τ is the cluster optical depth with respect to the Thomson scattering proces. The dependence from the non dimensional frequency, is entirely described by;

$$g(x) = \frac{x^4 e^x}{(e^x-1)} \left[x \frac{e^x+1}{e^x-1} - 1 \right] \quad (10)$$

Eq. 10 shows that the distortion is negative at low frequencies below the critical crossover value x_0 "" 3.83 (corresponding to ~ 217GHz) and positive in the high frequency region. Typical values of the y parameter are ~ 10^{-4} in rich and/or moderately hot clusters; from the corresponding expression for the CMB temperature fluctuation induced from the effect,

$$\frac{\Delta T_{CMB}}{T_{CMB}} = \left[x \frac{e^x+1}{e^x-1} - 4 \right] y \quad (11)$$

and being the spectral function of order unity, one gets for the induced CMB anisotropy a value of $\Delta T_{CMB}/T_{CMB} \approx 10^{-4}$, indicating that the thermal SZ effect (especially when compared to the primary CMB anisotropy power spectrum at high ls) is the dominating anisotropy observable in the direction of an even moderately rich and warm galaxy cluster. In the above calculation of the comptonization parameter, the angular separation from the cluster center has been inserted by means of well known transformation $r \approx \theta D_A$ which makes use of the angular diameter distance D_A. All the clusters have been set at the same Angular Distance (~ 20 arcmin), comparable with the total field of bolometer array (~ 17arcmin), to a resolution of 4.5'/pixel. We use in this simulation the temperature profile of the Eq. 1 and Eq. 2 for all the cluster that show a CF center. The Tab. 6 is equal with Tab. 5, but now the comptonization parameter Y_0 obtained from the SZ observation have been included

3. ΔI and ΔT_{CMB}

We have also built simulations of the change on the intensity of the CMB that crosses through the cluster ICM. To build these maps we have followed the same reasoning for the maps in comptonization parameter y_0. First we remember how much is this change in the intensity and in the temperature of the CMB for the changing in the intensity using this relation:

$$\Delta I_t = i_0 y g(x) \quad (12)$$

$$i_0 = \frac{2(kT_{CMB})^3}{(hc)^2} \quad (13)$$

$$g(x) = \frac{x^4 e^x}{(e^x-1)} \left[x \frac{e^x+1}{e^x-1} - 4 \right] \quad (14)$$

but now we have included in the calculations for the maps, also the relativistic effect for the clusters with a temperature of the electronic gas superior to (T_e > 10keV). In the same method we simulated the change on the temperature of CMB radiation, when it crosses the ICM matter of the cluster. Above we set the comptonization parameter (Eq. 9), the difference in temperature is defined above (§2) and we can remember now:

$$\frac{\Delta T_{CMB}}{T_{CMB}} = \left[x \frac{e^x+1}{e^x-1} - 4 \right] y \quad (15)$$

What it becomes

$$\Delta T_{CMB} = \left[x \frac{e^x+1}{e^x-1} - 4 \right] y T_{CMB} \quad (16)$$

For all this clusters we have included the relativistic corrections. We can see that, for some clusters we do not need relativistic corrections, the corrections on the ΔI are minimal (less than < 5%). First we show an sample of clusters (see Fig. 4), that represent one comparison with the SZ measurements, obtained from the SuZIE II observation (Benson et al., 2004), the data corresponds at three frequencies v_1, 2, 3 = 150GHz, 220GHz, 270GHz each. In the Fig. 5, we show the simulation on an sample of clusters for the ΔT versus adimensional frequencies $X=h\nu/kT_{CMB}$ in comparison with SZ data in ΔT provided from NOBEYAMA (one data Abell 773) (Tsuboi et al., 2004) and OVRO/BIMA observations (Bonamente et al., 2006).

4. RESULTS

In order to calculate the S-Z effect on the CMB, the change on the Intensity and the Temperature of the CMB passing through the ICM, we use a different model, the Cooling Flow model (Piffaretti et al., 2005), (Gitti et al., 2007), for the electronic gas temperature instead of Isothermal model. Although we use the beta model for the gas density (Cavaliere and Fusco-Femiano, 1976), (Cavaliere and Fusco-Femiano, 1978). For two clusters it's used the double-beta model (Mohr et al., 1999) Temperature profile is modelled by the equations 1 and 2. For the density profile is used equation 3 and the equation 4. Fig 2 show the best fit to the data available (X-Ray data Bonamente et al. (2006), LaRoque et al. (2006), Peterson et al. (2001)), for the temperature profile of the clusters sample. The Fig. 2 show the best fit for the density using double-β model (2 clusters), for all the other clusters the single-β model model has been used (one example of 2 clusters is showed in Fig 2). In order to obtain the best fitting temperature profile we fix the parameter μ = 2, the temperature $T_0$is set equal to the temperature of the central bin. For two clusters; Abell1835 and Abell2390 we provide also the slope parameter β, all other parameters are shown in the Tab. 2. The density parameters are shown in the Tab. 3, for the best fit

parameters we provide r_c in the case of three clusters; Abell1975, Abell1835 and Abell2390. For the double-β model we calculated both parameters; β_1, β_2 and r_{c1}, r_{c2} for the clusters Abell2204 and Abell2390. We can see the difference between these models are shown in the Fig. 2, while, in the Tab. 4 we can see the difference in the terms of χ^2, smaller in the case of the double-β, ten times than single-β model. Do to the lack of density data for the other clusters, we just use the single-β model, using the central density n_0, Tab. 3.

4.1. Y and ΔI, ΔT_{CMB} results

I derive the Comptonization parameter applying the equation:

$$y = \int_{l.o.s} n_e(l) \frac{kT_e}{m_e c^2} \sigma_T dl = \frac{kT_e}{m_e c^2} \tau \qquad (17)$$

where the temperature T_e and the density n_e are defined in the §2. We can see the results in the Tab. 5 and Tab. 6. In Table 5 it's shown the comptonisation parameter y_0 for 10 CF clusters, also three more cluster with no apparent CF profile has been include (on the third column), in order to provide a complete view for the analysis. the second column show the comptonisation parameter y_0 that isothermal model yield for these clusters. For the cluster MS 1358.4 the two model differ in the value, isothermal model y_0, is greater more than 60% than CF temperature profile model. For the cluster RXJ1374 the difference is much smaller < 4%, for the other 7 clusters the isothermal model overestimate the comptonisation parameter ∼ 20 ÷ 100%. The remaining clusters with a T_e temperature profile different from the isothermal model the change is smaller than 10%. Table 6 show the same results, but in this case we included the Y_0 yielded from the S-Z observations, see Zemcov et al. (2007), Benson et al. (2004), unfortunately only for 8 clusters. For the cluster Abell773, the CF profile fit very good with S-Z data, the isothermal model on the other hand, overestimate y_0 more than 50%, RXJ1347 S-Z observation fit both models, but isothermal profile is in a better agreement with S-Z data. In the case of ZW3146 both models do not agree with S-Z observations, both models overestimate y_0, CF profile model is much more near the observed value, while the isothermal model value, is 2.5 time greater than observed value. Abell1835 comptonisation model value it's only 15% smaller than S-Z observed value, Isothermal model value in the other hand it's 2 times greater, For Abell2204 we have a value for the comptonisation bigger than S-Z value, 2 and 3.5 times respectively. For the last cluster Abell2390 CF model value fit the S-Z data, while the Isothermal model overestimate y_0 by about two times. The ongoing step, simulating the changing in intensity and the temperature of CMB using the X-Ray data. The change in the intensity is given by:

$$\Delta I_t = i_0 y g(x) \qquad (18)$$

With the dependency from non dimensional frequency described by eq.8. While the change in the temperature is given by:

$$\Delta T_{CMB} = \left[x \frac{e^x + 1}{e^x - 1} - 4 \right] y T_{CMB} \qquad (19)$$

The resulting simulations are shown in the Fig.4 and Fig.5, for the change in intensity and temperature re- spectively. Observation from S-Z measurements are included (see Fig. 4), corresponding at three frequencies, $\nu_{1,2,3}$ = 150GHZ, 220GHz, 270GHz each, for the Intensity. Fig. 5 show the comparison between the simu- lations and the observed temperature change. ΔI simulations fit S-Z data very well for the central frequency in almost all the clusters, except Abell697, CL0016, but still within error bars. For the other two frequencies the simulation agree sufficiently for 2 clusters Abell1835 and ZW3146. In three other clusters the simulation fit the upper frequency; Abell773, CL0016 and RXJ1347. It seems that for ZW3146 the simulation fit sufficiently the data we have. In the case of ΔT the simulations fit the data for at least three clusters; A773, CL0016 and RXJ1347, for the other 6 clusters the simulations and the data are at the same order of magnitude.

5. CONCLUSION

In this paper we investigate the possibility of a new error in to calculate the Compton inverse effect (known as S- Z effect) on the CMB radiation, induced by the use of the Isothermal model, profiling the temperature of the hot electronic plasma, residing inside the gravitational weil of the clusters of galaxies. I used a different approach for the temperature profile, the Cooling Flow profile, using Eq.1 and Eq.2. We build the temperature profile of 12 clusters with X-ray data observation. In order to have a good view we calculated the Comptonisation parameter from both models and compared the results with S-Z data provided from the observations. We also simulated the change in ΔI and ΔT. We find out that, the CF temperature profiles differ from those obtained using the isothermal model. In the most cases the isothermal model overestimate the Comptonisation parameter, therefore introducing a new error into calculating cosmological parameters derived from combined observations; S-Z and X-ray. The difference between temperature profile models covers a wide range from 4% RXJ1347 to 100% Abell1795, Abell1835. When we fit these profiles with S-Z data y_0, the difference with the isothermal temperature profile model becomes even greater, for Abell2204 about 3.5 times. What we can tell is that for the clusters that shown this feature (CF), the new model reflects better the real condition of the hot electronic plasma that reside on the center of the clusters of galaxies. Given that, however we can see from the comparison of y_0 and the simulations on the intensity and temperature change, we have a discrepancy between simulated data from X-ray observations with those obtained from the direct S-Z observations.

References

[1] R. A. Sunyaev and Y. B. Zeldovich. Distortions of the Background Radiation Spectrum. , 223:721–722, August 1969. doi: 10.1038/223721a0.

[2] R. A. Sunyaev and Y. B. Zeldovich. The Observations of Relic Radiation as a Test of the Nature of X-Ray Radiation from the Clusters of Galaxies. Comments on

Astrophysics and Space Physics, 4:173, November 1972.

[3] M. Birkinshaw. Measurement of the Sunyaev-Zel'dovich Effect. In A. Blanchard, L. Celnikier, M. Lachieze- Rey, and J. Tran Thanh Van, editors, Physical Cosmology, page 177, 1991.

[4] M. Birkinshaw. The Sunyaev-Zel'dovich effect. , 310:97–195, March 1999. doi: 10.1016/S0370-1573(98)00080-5.

[5] J. E. Carlstrom, M. Joy, and L. Grego. Interferometric Imaging of the Sunyaev-Zeldovich Effect at 30 GHz. , 456:L75, January 1996. doi: 10.1086/309866.

[6] L. Grego, J. Carlstrom, M. Joy, and W. Holzapfel. The

[7] Sunyaev–Zel'dovich Effect Imaged in Galaxy Clusters. In American Astronomical Society Meeting Abstracts, volume 28 of Bulletin of the American Astronomical Society, page 115.05, December 1996.

[8] R. Piffaretti, P. Jetzer, J. S. Kaastra, and T. Tamura. Temperature and entropy profiles of nearby cooling flow clusters observed with XMM-Newton. , 433:101–111, April 2005. doi: 10.1051/0004-6361:20041888.

[9] R. Piffaretti and J. S. Kaastra. Effervescent heating: constraints from nearby cooling flow clusters observed with XMM-Newton. , 453:423–431, July 2006. doi: 10.1051/0004-6361:20054365.

[10] M. Gitti, R. Piffaretti, and S. Schindler. Mass distribution in the most X-ray-luminous galaxy cluster RX J1347.5-1145 studied with XMM-Newton. , 475:441–441, November 2007. doi: 10.1051/0004-6361:20077580e.

[11] M. F. Struble and H. J. Rood. A Compilation of Redshifts and Velocity Dispersions for ACO Clusters. , 125: 35–71, November 1999. doi: 10.1086/313274.

[12] J. T. Stocke, S. L. Morris, I. M. Gioia, T. Maccacaro, R. Schild, A. Wolter, T. A. Fleming, and J. P. Henry. The Einstein Observatory Extended Medium-Sensitivity Survey. II - The optical identifications. , 76:813–874, July 1991. doi: 10.1086/191582.

[13] A. Luppino and I. M. Gioia. Constraints on cold dark matter theories from observations of massive x-ray-luminous clusters of galaxies at high redshift. , 445:L77–L80, June 1995. doi: 10.1086/187894.

[14] M. Gioia and G. A. Luppino. The EMSS catalog of X-ray-selected clusters of galaxies. 1: an atlas of CCD images of 41 distant clusters. , 94:583–614, October 1994. doi: 10.1086/192083.

[15] S. W. Allen, A. C. Edge, A. C. Fabian, H. Bohringer, C. S. Crawford, H. Ebeling, R. M. Johnstone, T. Naylor, and R. A. Schwarz. Optical spectroscopy of the ROSAT X-ray brightest clusters. , 259:67–81, November 1992.

[16] D. Clemens, M. Berkovitch, J. Yun, N. Patel, and T. Xie. The Outflow; Dense Core; and "Jet" in L810. In D. P. Clemens and R. Barvainis, editors, Clouds, Cores, and Low Mass Stars, volume 65 of Astronomical Society of the Pacific Conference Series, page 386, 1994.

[17] S. W. Allen, R. W. Schmidt, and A. C. Fabian. The X-ray virial relations for relaxed lensing clusters observed with Chandra. , 328:L37–L41, December 2001. doi: 10.1046/j.1365-8711.2001.05079.x.

[18] P. Mazzotta, E. Rasia, S. Borgani, L. Moscardini, K. Dolag, and G. Tormen. Spectroscopic-Like Temperature of Clusters of Galaxies and Cosmological Implications. ArXiv Astrophysics e-prints, December 2004.

[19] J. J. Mohr, B. Mathiesen, and A. E. Evrard. Properties of the Intracluster Medium in an Ensemble of Nearby Galaxy Clusters. , 517:627–649, June 1999. doi: 10.1086/307227.

[20] A. Cavaliere and R. Fusco-Femiano. X-rays from hot plasma in clusters of galaxies. , 49:137–144, May 1976.

[21] Cavaliere and R. Fusco-Femiano. The Distribution of Hot Gas in Clusters of Galaxies. , 70:677, November 1978.

[22] M. Bonamente, M. K. Joy, S. J. LaRoque, J. E. Carlstrom, E. D. Reese, and K. S. Dawson. Determination of the Cosmic Distance Scale from Sunyaev-Zel'dovich Effect and Chandra X-Ray Measurements of High- Redshift Galaxy Clusters. , 647:25–54, August 2006. doi: 10.1086/505291.

[23] S. J. LaRoque, M. Bonamente, J. E. Carlstrom, M. K. Joy, D. Nagai, E. D. Reese, and K. S. Dawson. X-Ray and Sunyaev-Zel'dovich Effect Measurements of the Gas Mass Fraction in Galaxy Clusters. , 652:917–936, December 2006. doi: 10.1086/508139.

[24] T. Tamura, J. S. Kaastra, J. W. A. den Herder, J. A. M. Bleeker, and J. R. Peterson. Abundances in intracluster medium with XMM (Tamura+, 2004). VizieR Online Data Catalog, 342:135, July 2004.

[25] A S Kompaneets. Sov. Phys. JETP, (4):730, 1957. .

[26] M. Zemcov, C. Borys, M. Halpern, P. Mauskopf, and D. Scott. A study of the Sunyaev-Zel'dovich increment using archival SCUBA data. , 376:1073–1098, April 2007. doi: 10.1111/j.1365-2966.2007.11443.x.

[27] A. Benson, S. E. Church, P. A. R. Ade, J. J. Bock, K. M. Ganga, C. N. Henson, and K. L. Thompson. Measurements of Sunyaev-Zel'dovich Effect Scaling Relations for Clusters of Galaxies. , 617:829–846, December 2004. doi: 10.1086/425677.

[28] M. Tsuboi, A. Miyazaki, T. Kasuga, N. Kuno, A. Sakamoto, and H. Matsuo. Sunyaev–Zel'dovich Effect toward Distant Galaxy Clusters at 43 GHz; Observation and Data. , 56:711–721, October 2004.

[29] J. R. Peterson, F. B. S. Paerels, J. S. Kaastra, M. Arnaud, T. H. Reiprich, A. C. Fabian, R. F. Mushotzky, J. G. Jernigan, and I. Sakelliou. X-ray imaging-spectroscopy of Abell 1835. , 365:L104–L109, January 2001. doi: 10.1051/0004-6361:20000021.

[30] W. Pratt, H. Böhringer, J. H. Croston, M. Arnaud, S. Borgani, A. Finoguenov, and R. F. Temple. Temperature profiles of a representative sample of nearby X-ray galaxy clusters. , 461:71–80, January 2007. doi: 10.1051/0004-6361:20065676.

[31] R. W. Schmidt, S. W. Allen, and A. C. Fabian. Chandra observations of the galaxy cluster Abell 1835. , 327: 1057–1070, November 2001. doi: 10.1046/j.1365-8711.2001.04809.x.

[32] C. Stewart, A. C. Fabian, C. Jones, and W. Forman. The prevalence of cooling flows in clusters of galaxies. , 285:1–6, October 1984. doi: 10.1086/162470.

[33] Kaastra. High Spectral Resolution Observations of AGN. In XMM-Newton: The Next Decade, June 2007.

[34] W. Pratt, M. Arnaud, and N. Aghanim. An XMM-Newton Mosaic Observation of A2163. In S. Borgani,

[35] M. Mezzetti, and R. Valdarnini, editors, Tracing Cosmic Evolution with Galaxy Clusters, volume 268 of Astronomical Society of the Pacific Conference Series, page 433, 2002.

Appendix:

***Table 1**. Cluster sample.*

Cluster	Right ascension J2000.0	Declination J2000.0	z	
ABELL 773	09h17m59s	51.7064	0.217000 (1)	CF
MS 1358.4+6245	13h59m54.3s	62.5101	0.328000 (2)	CF
RXJ 1347				CF
ZW 3146	10h23m39.63s	4.18621	0.290600 (3)	CF
ABELL 1795	13h49m00s	26.5852	0.062476	CF
ABELL 1835	14h01m02s	2.8588	0.253200 (1)	CF (probably)
ABELL 2204	16h32m45s	5.5785	0.152158 (1)	CF
ABELL 2390	21h53m34s	17.6697	0.228000 (1)	CF

(1) Right ascension, Declination and z reference (Struble and Rood, 1999)
(2) Right ascension, Declination and z reference (Luppino and Gioia, 1995; Gioia and Luppino, 1994)
(3) Right ascension, Declination and z reference (Allen et al., 1992)

***Table 2**. R_C is the cooling radius obtained from the best fit parameters fitting temperature profile with Eqs. 1 and 2. Here, $\mu = 2$ in Eq. 1 is used and, for booth fitting functions, T_0 is set equal to the temperature of the central bin. The radius present in this table for the NON-CF cluster intends the radius, where the temperature decrease when i apply the Eqs. 1 and 2.*

Cluster	$R_{T,max}$ (kpc)	R_c (kpc)	T_0 (keV)	T_1 (keV)	β	
ABELL 697	450	26.2	10.1	1.24	0.587	NO-CF
ABELL 773	1500	291.4	6	6.79	0.564	CF
Cl 0016	700	233.1	11.2	-3.17	0.761	NO-CF
MS 0451.6	499	56	14.3	-4.95	0.777	NO-CF
MS 1054.4	474	73	13.8	-4.47	1.791	NO-CF
MS 1358.4	454	57	4.02	5.8	0.675	CF
RXJ 1347	1000	26	7.6	2.4	0.631	CF
ZW 3146	450	49	3.6	5.02	0.668	CF
ABELL 1795	800	45	5.73	3.5	0.52	CF
ABELL 1835	450	65	6	8.5	0.72 (3)	CF (probably)
ABELL 1995	573	160.35	7.8	1.2	1.298	NO-CF
ABELL 2163	2300	177.64	9	3.79	0.560	CF
ABELL 2204	200	72.86	3.1	6.6	0.710	CF
ABELL 2390	870	50.2	4.9	4.45	0.47 (3)	CF

(1) Density and temperature reference (CHANDRA) (LaRoque et al., 2006).
(2) Density and temperature reference (CHANDRA) (Tamura et al., 2004)
(3) This paper.

β-reference (Bonamente et al., 2006)

Table 3. *R_C for the density profile that are used to fit the data. Also β, β_1 and β_2 for the double-β model including r_{c1} and r_{c2} (CHANDRA).*

Cluster	r_c (kpc)	β	n_0 $x10^{-3}$	β_1	β_2	r_{c1} (kpc)	r_{c2} (kpc)
ABELL 697	117	0.59	$9.82^{+1.55}_{-1.28}$x10-3 (1)				
ABELL 773	136	0.56	$8.04^{+0.68}_{-0.64}x10^{-3}$(1)				
Cl 0016	180	0.76	$1.4^{+0.0018}_{-0.0015}$x10-2 (1)				
MS 0451.6	205	0.77	$1.26^{+0.12}_{-0.09}x10^{-2}$(1)				
MS 1358.4	137	0.67	$9.62^{+0.78}_{-0.78}x10^{-2}$(1)				
RXJ 1347	138	0.63	$2.81^{+0.016}_{-0.012}x10^{-1}$(1)				
ZW 3146	110	0.67	$1.7^{-0.02}_{-0.03}x10^{-1}$(1)				
ABELL 1795	38(3)	0.52(3)	0.05 (2)				
ABELL 1835	65(3)	0.72 (3)	$1.1^{+0.05}_{-0.02}x10^{-1}$(1)				
ABELL 1995	360	1.3	$9.35^{+0.74}_{-0.56}x10^{-3}$(1)				
ABELL 2204	160	0.71	$2.01^{+0.12}_{-0.09}x10^{-1}$(1)	0.55(3)	1.43(3)	17.1(3)	7.1(3)
ABELL 2390	35(3)	0.47 (3)	0.8 (2)	0.35(3)	2.38(3)	23(3)	7.5(3)

(1) R_c, density and β reference (LaRoque et al., 2006)
(2) Density reference (Tamura et al., 2004) (CHANDRA).
(3) This paper.

Table 5. *In this table I show the comptonization parameter for the cluster in question. For the cluster with cooling flow (CF) has been obtained applying the temperature profile see Eqs. 1 and 2. For a complete view of the effect I apply Eqs. 1 and 2 for all clusters.*

Cluster	y0 (CF)	y0 (Isothermal)	y0 ($T_e$profile)	
ABELL 697	–	$1.4x10^{-4}$	–	NO-CF
ABELL 773	$4.5x10^{-4}$	$7.06x10^{-4}$	–	CF
Cl 0016	–	$4.32x10^{-4}$	$3.44x10^{-4}$	NO-CF
MS 0451.6	–	$2.99x10^{-4}$	$2.85x10^{-4}$	NO-CF
MS 1358.4	$7.88x10^{-4}$	$12.8x10^{-4}$	–	CF
RXJ 1347	$9.18x10^{-4}$	$9.52x10^{-4}$	–	CF
ZW 3146	$6.2x10^{-4}$	$9.1x10^{-4}$	–	CF
ABELL 1795	8.02^{-6}	$1.5x10^{-5}$	–	CF
ABELL 1835	$6.28x10^{-4}$	$1.31x10^{-3}$	–	CF
ABELL 1995	$8.52x10^{-5}$	$9.82x10^{-5}$	–	Uncertain
ABELL 2204	$5.3x10^{-4}$	$8.11x10^{-4}$	–	CF
ABELL 2390	$3.99x10^{-4}$	$6.18x10^{-4}$	–	CF

Table 6. *The same table, but this time comptonization parameters obtained from SZ observations, has been included.*

Cluster	y0 (CF)	y0 (Isothermal)	y0 ($T_e$profile)	Y_0 (SZ observation)
ABELL 697	–	$1.44x10^{-4}$	–	–
ABELL 773	$4.5x10^{-4}$	$7.06x10^{-4}$	–	$4.23x10^{-4}$(2)
Cl 0016	–	$4.32x10^{-4}$	$3.44x10^{-4}$	$3.27x10^{-4}$(2)
MS 0451.6	–	$2.99x10^{-4}$	$2.85x10^{-4}$	$2.84x10^{-4}$(2)
MS 1358.4	$7.88x10^{-4}$	$12.8x10^{-4}$	–	
RXJ 1347	$9.18x10^{-4}$	$9.52x10^{-4}$	–	$10.65x10^{-4}$(2)
ZW 3146	$6.2x10^{-4}$	$9.1x10^{-4}$	–	$3.62x10^{-4}$(2)
ABELL 1795	$8.02x10^{-6}$	$1.5x10^{-5}$	–	–
ABELL 1835	$6.28x10^{-4}$	$1.31x10^{-3}$	–	$7.66x10^{-4}$(2)
ABELL 1995	$8.52x10^{-5}$	$9.82x10^{-5}$	–	$8.58x10^{-5}$
ABELL 2204	$5.3x10^{-4}$	$8.11x10^{-4}$	–	$2.53x10^{-4}$(2)
ABELL 2390	$3.99x10^{-4}$	$6.18x10^{-4}$	–	$3.56x10^{-4}$(2)

(1) Scuba data Zemcov et al. (2007).
(2) SuZIE II dataBenson et al. (2004)

***Fig. 1**. The best fit-profiles of temperature for the clusters: MS 1358, ZW3146 and RXJ1120 (cooling flow).*

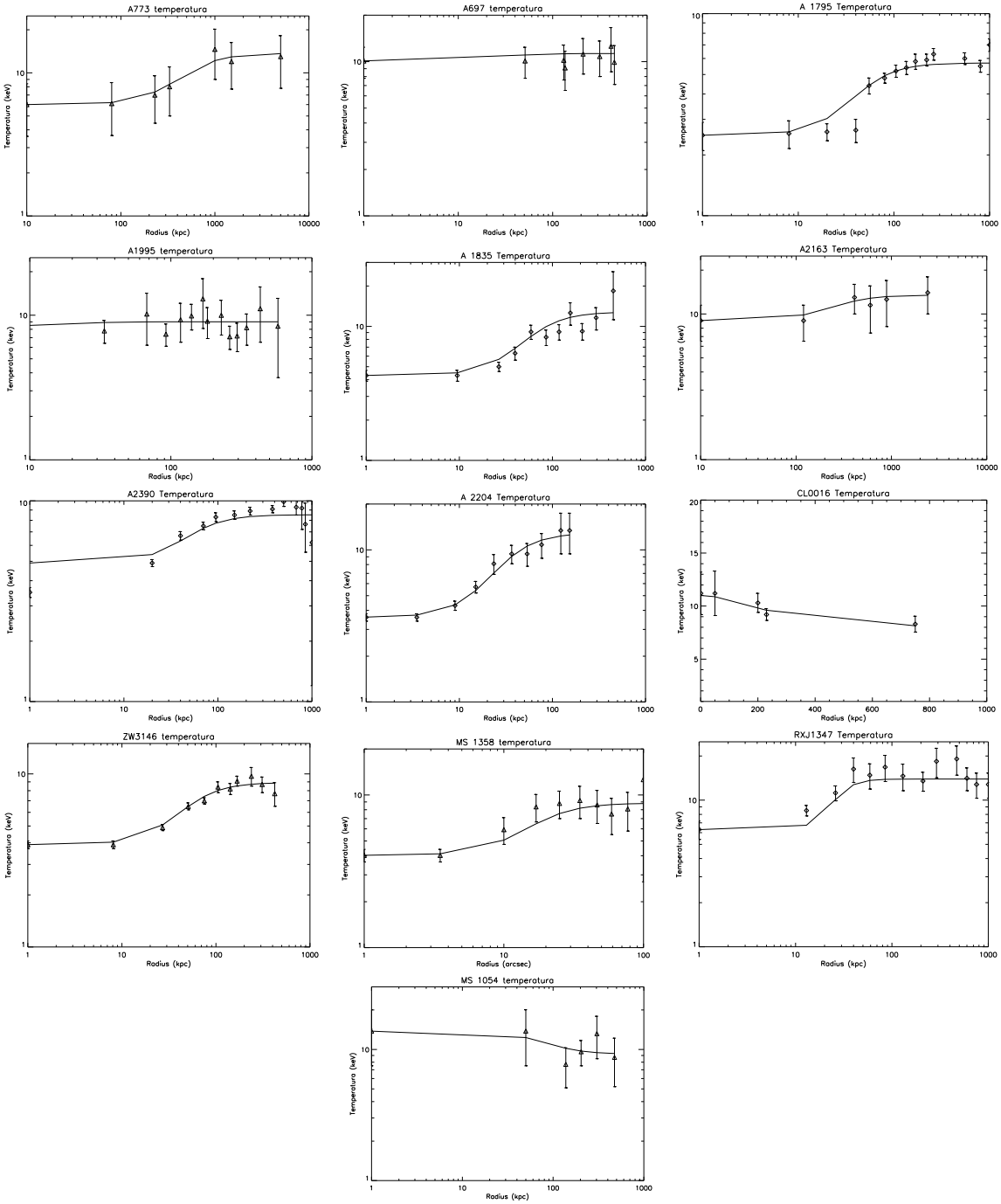

***Fig. 2**. β-model is applied to fit the density profile for the clusters: A1795 and A1835.*

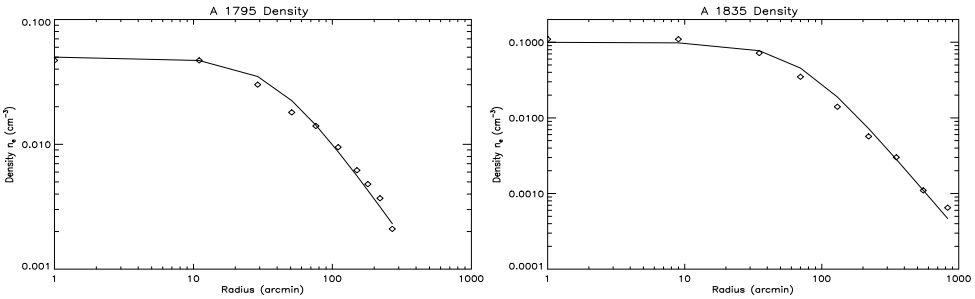

Fig. 3. *Abell 2204 and Abell 2390 density profile (comparison between β and double β model).*

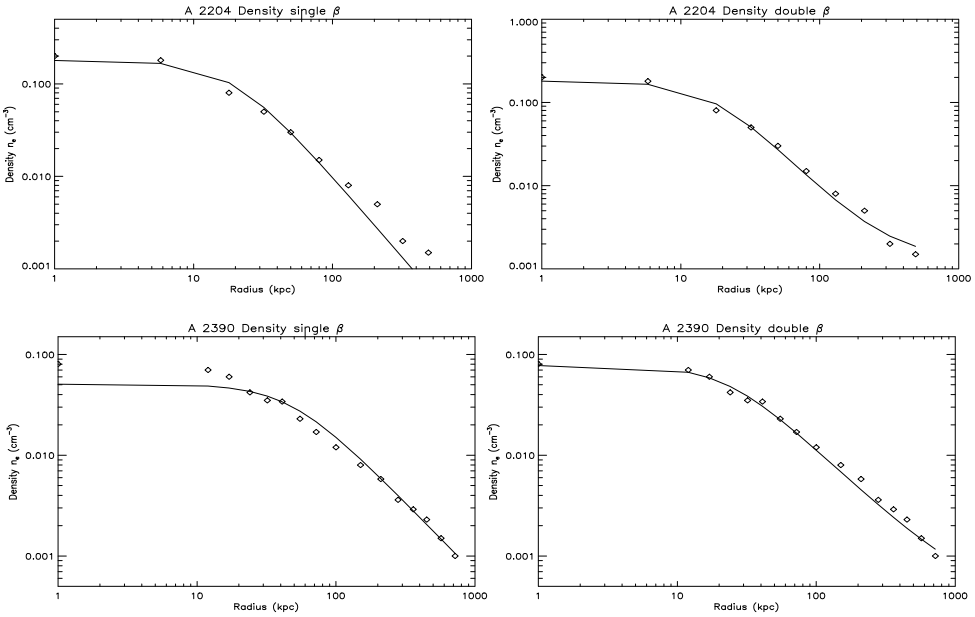

Fig. 4. *ΔI of the CMB radiation crossing the ICM matter of the clusters, to the adimensional frequency x*

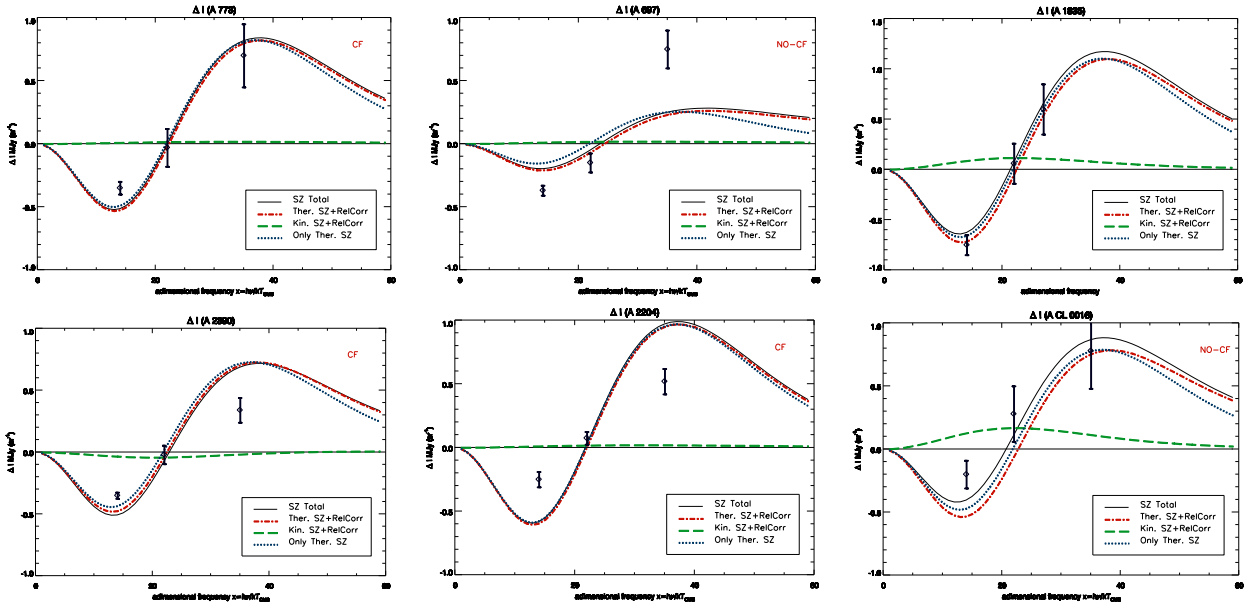

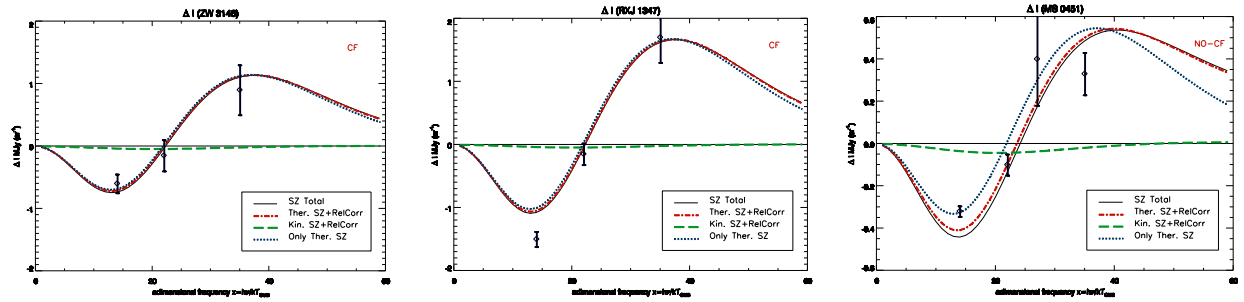
CF
NO−CF
SZ Total
Ther. SZ+RelCorr
Kin. SZ+RelCorr
Only Ther. SZ

Fig. 5. *ΔT.*

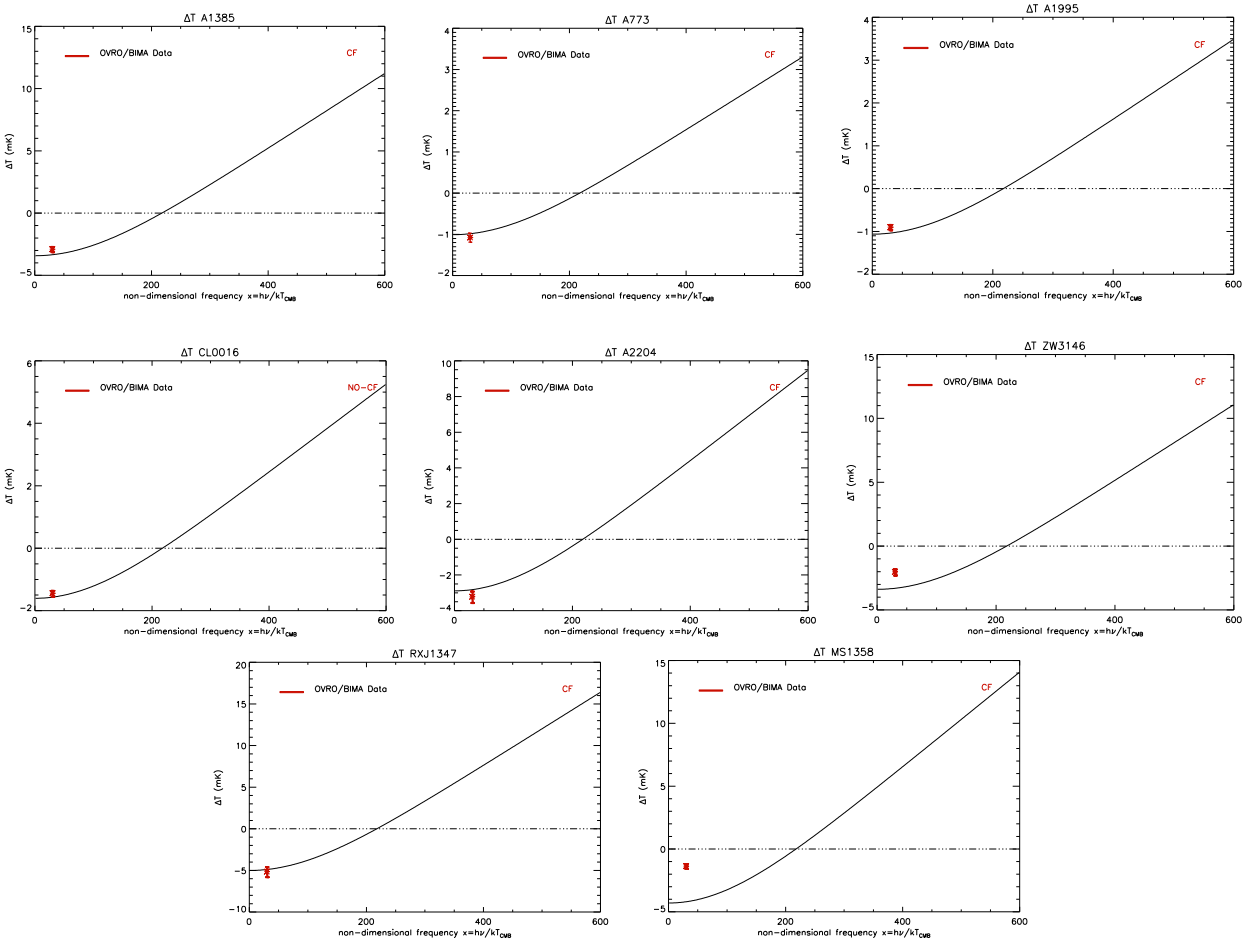
ΔT A1385
ΔT A773
ΔT A1995
ΔT CL0016
ΔT A2204
ΔT ZW3146
ΔT RXJ1347
ΔT MS1358
OVRO/BIMA Data
CF
NO−CF
ΔT (mK)
non−dimensional frequency x=hν/kT_CMB